ELSEVIER

Agricultural and Forest Meteorology 81 (1996) 299–323

AGRICULTURAL AND FOREST METEOROLOGY

# Estimating temperature of mulched and bare soil from meteorological data

Yihua Wu [a], Katharine B. Perry [b,*], Jean B. Ristaino [c]

[a] *The Climate Department, State Meteorological Administration, Beijing, 100081, People's Republic of China*
[b] *Department of Horticultural Science, North Carolina State University, Raleigh, NC 27695-7609, USA*
[c] *Department of Plant Pathology, North Carolina State University, Raleigh, NC 27695-7616, USA*

Received 21 April 1994; accepted 26 October 1995

**Abstract**

In order to investigate the application potential for soil solarization in the southern US without conducting labor intensive field tests and expensive experiments, a numerical model has been developed to estimate the temperature profile of both mulched and bare soils. Atmospheric and soil conditions, as well as the transmissivity, reflectivity and emissivity of mulch are considered in the model. The required dynamic inputs are hourly measurements of global radiation, air temperature, dewpoint, wind speed and rainfall.

The model was validated using hourly observations from 12 contiguous days of July 6–18, 1990 at the North Carolina State University Horticultural Crops Research Station near Clinton. Different weather occurred during the period. The model worked very well on both clear and rainy days except July 17 when large, rapid changes of the air temperature and solar radiation occurred. However, the percentages of the absolute differences less than 2.0°C between the hourly estimated and measured soil temperatures at 10, 20, and 30 cm were 89, 95 and 95 for mulched soil, and 94, 98 and 100 for bare soil, respectively. The correlation between estimated and measured temperatures yielded R-square values between 0.82 and 0.93. The model was very successful to satisfy the main objectives in this study. Model sensitivities to 23 parameters were analyzed. Relative sensitivity coefficients were higher for soil bulk density, quartz fraction, and mulch transmissivity to solar radiation, than for surface roughness length, soil clay fraction and mulch transmissivity to long wave radiation.

* Corresponding author.


*SSDI* 0168-1923(95)02320-8

## 1. List of symbols

| | |
|---|---|
| $a_s$ | the soil albedo |
| $C$ | the volumetric heat capacity of soil ($J\,m^{-3}\,K^{-1}$) |
| $C_p$ | the volumetric heat capacity of air ($J\,m^{-3}\,K^{-1}$) |
| $D$ | the soil thermal diffusivity ($m^2\,s^{-1}$) |
| $e_a$ | vapor pressure of the air (Pa) |
| $f'(T^n)$ | the derivative of the function $f(T^n)$ evaluated at $T^n$. |
| $F_i$ | the volume fractions of air, clay, organic matter, quartz and water in the soil |
| $\boldsymbol{G}$ | the soil heat flux ($W\,m^{-2}$) |
| $g_i$ | the shape factor of the granule of the soil |
| $\boldsymbol{H}$ | the sensible heat flux ($W\,m^{-2}$) |
| $h_i$ | the heat transfer coefficient ($W\,m^{-2}\,K^{-1}$) inside the mulch |
| $h_o$ | the heat transfer coefficient ($W\,m^{-2}\,K^{-1}$) outside the mulch |
| $K_i$ | the weighting factors of air, clay, organic matter, quartz and water in the soil |
| $L$ | the latent heat of vaporization ($J\,kg^{-1}$) |
| $m$ | Van Genuchten parameter |
| $n$ | Van Genuchten parameter |
| $P_1$ | the soil water pressure potential head of the surface layer (m) |
| $q_a$ | air humidity ($kg\,m^{-3}$) |
| $q_o$ | the saturation humidity of the surface layer ($kg\,m^{-3}$) |
| $q_s$ | the air humidity in the soil surface layer ($kg\,m^{-3}$) |
| $\boldsymbol{R}_a$ | the atmospheric long wave radiation ($W\,m^{-2}$) |
| $r_a$ | the aerodynamic resistance ($s\,m^{-1}$) |
| $\boldsymbol{R}_n$ | the net radiation flux ($W\,m^{-2}$) |
| $\boldsymbol{R}_s$ | the measured global radiation ($W\,m^{-2}$) |
| $r_s$ | the surface resistance ($s\,m^{-1}$) |
| $T$ | soil temperature (K) |
| $t$ | time (s) |
| $T_a$ | air temperature (K) |
| $T_d$ | dewpoint temperature (°C) |
| $T_m$ | the mulch temperature (K). |
| $u$ | wind speed ($m\,s^{-1}$) |
| $z$ | soil depth (m) |
| $\alpha$ | Van Genuchten parameter ($10^{-4}\,Pa^{-1}$) |
| $\delta$ | the difference operator |
| $\epsilon_s$ | the soil emissivity ($W\,m^{-2}$) |
| $\lambda$ | the soil thermal conductivity ($W\,m^{-1}\,K^{-1}$) |
| $\boldsymbol{\lambda E}$ | the latent heat flux ($W\,m^{-2}$) |
| $\theta$ | the actual water content of the surface layer ($m^3\,m^{-3}$) |
| $\theta_r$ | the residual water content of the surface layer ($m^3\,m^{-3}$) |
| $\theta_s$ | the saturated water content of the surface layer ($m^3\,m^{-3}$) |
| $\rho_1$ | the reflectivity of the mulch to long wave radiation |

| | |
|---|---|
| $\rho_s$ | the reflectivity of the mulch to solar wave radiation |
| $\sigma$ | the Stefan–Boltzmann constant ($5.67 \times 10^{-8}$ W m$^{-2}$ K$^{-4}$) |
| $\tau_l$ | the transmissivity of the mulch to long wave radiation |
| $\tau_s$ | the transmissivity of the mulch to solar wave radiation |

## 2. Introduction

Soil solarization which has been a relatively simple, effective, economical and nonchemical approach to soil disinfestation in hot, arid areas since the 1970s (Katan and DeVay, 1991) relies on elevating soil temperatures to a level that kills both pathogenic and beneficial microbes in the soil. Research on integrated control of *Sclerotium rolfsii* on tomato and pepper using solarization and biological control has been conducted for five years in North Carolina (Ristaino et al., 1991). The treatment of solarized soils with the beneficial biocontrol fungus *Gliocladium virens* could provide an additional management alternative for southern blight in the coastal plains of the southeast US. A model predicting both bare and mulched soil temperature will assist in determining the potential application of solarization in this region. Such a model could also serve as an effective tool in lieu of an expensive network of observations in wide range of locations.

Several types of soil temperature models have been developed. Mahrer (1979), Mahrer and Katan (1981), Cenis (1989) and Sui et al. (1992) developed models to predict mulched soil temperature. The model described in Mahrer (1979) and Mahrer and Katan (1981) is physically based and is general in application potential. However, its application is limited by requiring radiosonde data or bare soil temperature data which are not available at most meteorological stations. The Cenis (1989) model uses Fourier methodology to simulate the daily sinusoidal change of temperature in a homogeneous soil. Because its input requirements are daily maximum and minimum soil temperatures at two depths, its application is site specific. The model by Sui et al. (1992) can simulate soil temperature and moisture profiles under various mulches which were classified into two categories: porous mulches (e.g. straw, gravel, sand) and film mulches (e.g. oiled paper, asphalt emulsion film, etc.). However, rainfall, a very important element affecting both energy balance and water balance, was not considered, and the sum of the mulch transmissivity, reflectivity and emissivity used in their study is greater than unity.

Ten Berge (1990) and Horton and Chung (1991) developed models to predict bare soil temperature based on theory similar to Mahrer (1979) and Mahrer and Katan (1981). The required weather inputs for the Ten Berge (1990) model are data at 30 min intervals of solar radiation, vapor pressure, air temperature, wind speed and rainfall. The Horton and Chung (1991) model requires daily global radiation, maximum and minimum air temperature, average wind speed and total rainfall. These data are available at most meteorological stations. However, these models do not estimate mulched soil temperature.

The objective of this study was to develop a physically based model which uses easily accessed meteorological data to predict temperatures of both bare and mulched soils to provide information for further assessment of the application of solarization in the southern US.

## 3. Model description

A 3 meter soil profile was divided into 33 sublayers. The soil temperatures in all layers (depths) except the top and bottom were calculated by the following heat transfer equation. The top layer temperature is determined by energy budget analysis at the soil surface. The bottom layer temperature is assumed to be constant.

$$C\frac{\delta T}{\delta t} = \frac{\delta\left(\lambda\frac{\delta T}{\delta z}\right)}{\delta z} \tag{1}$$

where $C$ is the volumetric heat capacity of soil (J m$^{-3}$ K$^{-1}$), $\delta$ is the difference operator, $T$ is soil temperature (K), $t$ is time (s), $z$ is soil depth (m), and $\lambda$ is the soil thermal conductivity (W m$^{-1}$ K$^{-1}$).

The soil volumetric heat capacity ($C$) and the soil thermal conductivity ($\lambda$) are determined as in De Vries (1963) and Ten Berge (1990) as follows.

$$C = \Sigma C_i F_i \tag{2}$$

where $C_i$ is the volumetric heat capacity and $F_i$ the volume fraction of soil components air, clay, organic matter, quartz and water, respectively.

$$\lambda = \frac{\Sigma K_i F_i \lambda_i}{\Sigma K_i F_i} \tag{3}$$

where $K_i$ is the weighting factor and $\lambda_i$ the thermal conductivity of each soil component. De Vries (1963) suggested that soil can be considered to be composed of spheroids. Under this assumption, the following equation is used to determine $K_i$:

$$K_i = \tfrac{2}{3}\left[1 + \left(\frac{\lambda_i}{\lambda_0} - 1\right)g_i\right] + \tfrac{1}{3}\left[1 + \left(\frac{\lambda_i}{\lambda_0} - 1\right)(1 - 2g_i)\right] \tag{4}$$

where $\lambda_0$ is the 'medium' thermal conductivity, $g_i$ is the so-called 'shape factor' which accounts for the shape of the granule and its orientations with respect to the three axes of physical space.

The energy budget at the soil surface determines the upper boundary conditions of the model, which drive the entire model. The surface energy budget is given by

$$\boldsymbol{R}_\mathrm{n} + \boldsymbol{H} + \boldsymbol{\lambda E} + \boldsymbol{G} = 0 \tag{5}$$

where $\boldsymbol{R}_\mathrm{n}$ is the net radiation flux, $\boldsymbol{H}$ is the sensible heat flux, $\boldsymbol{\lambda E}$ is the latent heat flux, and $\boldsymbol{G}$ is the soil heat flux, all in W m$^{-2}$. These parameters are different at the bare soil surface, the mulched soil surface and the surface of the mulch.

### 3.1. Bare soil surface

The net radiation flux at the bare soil surface is given by:

$$\boldsymbol{R}_\mathrm{n} = \underset{\mathrm{A}}{(1 - a_\mathrm{s})\boldsymbol{R}_\mathrm{s}} + \underset{\mathrm{B}}{\epsilon_\mathrm{s}\boldsymbol{R}_\mathrm{a}} - \underset{\mathrm{C}}{\epsilon_\mathrm{s}\sigma T^4} \tag{6}$$

where $a_\mathrm{s}$ is the soil albedo, $\boldsymbol{R}_\mathrm{s}$ is the measured global radiation, $\epsilon_\mathrm{s}$ is the soil emissivity, $\boldsymbol{R}_\mathrm{a}$ is the atmospheric long wave radiation, and $\sigma$ is the Stefan–Boltzmann constant ($5.67 \times 10^{-8}$ W m$^{-2}$ K$^{-4}$). The soil albedo ($a_s$), the soil emissivity ($\epsilon_s$), and the atmospheric long wave radiation ($\boldsymbol{R}_a$) are determined as in Van Bavel and Hillel (1976).

The three terms labled A, B, and C in Eq. (6) are the net short wave radiation and atmosphere long wave radiation absorbed by the bare soil surface, and long wave radiation emitted by the bare soil surface respectively. They are determined by the bare soil surface properties and conditions. For a given surface and wavelength, the sum of reflectivity, absorptivity and transmissivity equals unity. As the soil is considered to be an opaque body, it is assumed that the sum of its reflectivity and absorptivity to short (long) wave radiation equals unity. If the soil absorptivity of long wave radiation is further assumed to be its emissivity ($\epsilon_s$), term B $= \boldsymbol{R}_a - (1 - \epsilon_s)\boldsymbol{R}_a = \epsilon_s \boldsymbol{R}_a$.

The air humidity ($q_a$, kg m$^{-3}$) which is required to determine $\boldsymbol{R}_a$ is calculated using the equations from Chen and Jiang (1989):

$$q_a = 2.17 \times 10^{-3}\, e_a/T_a \tag{7}$$

$$e_a = 611 \times 10^{[7.45T_d/(235+T_d)]} \tag{8}$$

where $T_a$ is air temperature (K), $e_a$ is vapor pressure of the air (Pa), $T_d$ is dewpoint temperature (°C). Eq. (8) is Magnus' equation which is the most widely used by meteorologists (Murray, 1967). Chen and Jiang (1989) found that this equation gives the best agreement with experimental data.

The sensible heat flux in Eq. (5) is determined by:

$$\boldsymbol{H} = C_p(T_a - T)/r_a \tag{9}$$

where $C_p$ is the volumetric heat capacity of air (J m$^{-3}$ K$^{-1}$), and $\mathrm{r}_a$ is the aerodynamic resistance (s m$^{-1}$).

The aerodynamic resistance ($r_a$) is calculated from Van Bavel and Hillel (1976):

$$r_a = r_n S_t \tag{10}$$

$$S_t = 1/(1 - 10\mathrm{Ri}) \tag{11}$$

$$\mathrm{Ri} = 9.81(2 - z_o)(T_a - T)/(T_a u^2) \tag{12}$$

$$r_n = 6.25(\ln(2/z_o))^2/u \tag{13}$$

where $r_n$ is the adiabatic or neutral value of $r_a$, $S_t$ is the stability correction, Ri is the Richardson number, $z_o$ is the surface roughness length (m), and $u$ is wind speed (m s$^{-1}$), 2 is the height (m) at which wind speed was recorded.

The latent heat flux in Eq. (5) is determined as following:

$$\boldsymbol{\lambda E} = L(q_a - q_s)/(r_a + r_s) \tag{14}$$

where $L$ is the latent heat of vaporization (J kg$^{-1}$), $q_s$ is the air humidity in the soil surface layer (kg m$^{-3}$), and $r_s$ is the surface resistance (s m$^{-1}$).

The latent heat of vaporization ($L$) is calculated by the following equation used by Horton and Chung (1991):

$$L = 2.49463 \times 10^6 - 2.247 \times 10^3 \times (T - 273.16) \tag{15}$$

where $L$ is in J kg$^{-1}$.

The air humidity in the soil surface layer ($q_s$) is calculated by the following equations in Van Bavel and Hillel (1976) and Chen and Jiang (1989).

$$q_s = q_o \times \exp[P_l/(46.97 \times T)] \tag{16}$$

$$q_o = 2.17 \times 10^{-3}\ e_s/T \tag{17}$$

$$e_s = 611 \times 10^{[7.45T/(235+T)]} \tag{18}$$

where $P_l$ is the soil water pressure potential head of the surface layer (m), $q_o$ is the saturation humidity of the surface layer (kg m$^{-3}$), $e_s$ is the saturated water vapor pressure in the soil surface layer (Pa).

The soil water pressure potential head ($P_l$) is calculated as in Ten Berge (1990) by the following equation:

$$P_l = -\alpha^{-1}\left\{[(\theta - \theta_r)/(\theta_s - \theta_r)]^{-1/m} - 1\right\}^{1/n} \tag{19}$$

where $\alpha$, $m$ and $n$ are the so called 'Van Genuchten parameters', $\theta$, $\theta_r$ and $\theta_s$ are the actual, residual, and saturated water content of the surface layer respectively, all in m$^3$ m$^{-3}$. The residual water content is the water content when hydraulic conductivity $\to 0$.

The soil heat flux in Eq. (5) is determined as the function of soil temperature gradient as following:

$$\boldsymbol{G} = \lambda(\delta T/\delta z) \tag{20}$$

where $\lambda$ is the same as in Eq. (1).

### 3.2. Mulched soil surface

The net radiation flux at the mulched soil surface is determined as:

$$\begin{aligned} \boldsymbol{R}_n = {} & \underbrace{\boldsymbol{R}_s\tau_s(1-a_s)/(1-\rho_s a_s)}_{A} + \underbrace{\boldsymbol{R}_a\epsilon_s\tau_l/(1-\rho_l+\rho_l\epsilon_s)}_{B} \\ & + \underbrace{\epsilon_s\epsilon_m\sigma T_m^4/(1-\rho_l+\rho_l\epsilon_s)}_{C} - \underbrace{(1-\rho_l)\epsilon_s\sigma T^4/(1-\rho_l+\rho_l\epsilon_s)}_{D} \end{aligned} \tag{21}$$

where $\tau_s$, $\rho_s$, $\tau_l$, $\rho_l$ are transmissivity and reflectivity of the mulch to solar and long wave radiation, respectively; $\epsilon_m$ is the mulch emissivity, and $T_m$ is the mulch temperature (K).

The terms labeled A, B, C and D in Eq. (21) are the net short wave radiation, net atmosphere long wave radiation, and mulch long wave radiation absorbed by the mulched soil surface, and the long wave radiation from the mulched soil surface. These terms are determined by both mulch optical properties (transmissivity and reflectivity) and soil properties and conditions. For example, term A is affected by mulch transmissivity and reflectivity, and soil albedo which is affected by soil moisture. Considering the infinite transfer processes of short wave radiation under mulch (Fig. 1), term A is given by:

$$\begin{aligned} \text{Term A} = {} & \boldsymbol{R}_s\tau_s - \boldsymbol{R}_s\tau_s a_s + \boldsymbol{R}_s\tau_s a_s\rho_s - \boldsymbol{R}_s\tau_s a_s^2\rho_s + \boldsymbol{R}_s\tau_s a_s^2\rho_s^2 \\ & - \boldsymbol{R}_s\tau_s a_s^3\rho_s^2 + \boldsymbol{R}_s\tau_s a_s^3\rho_s^3 - \boldsymbol{R}_s\tau_s a_s^4\rho_s^3 + \boldsymbol{R}_s\tau_s a_s^4\rho_s^4 - \cdots. \end{aligned}$$

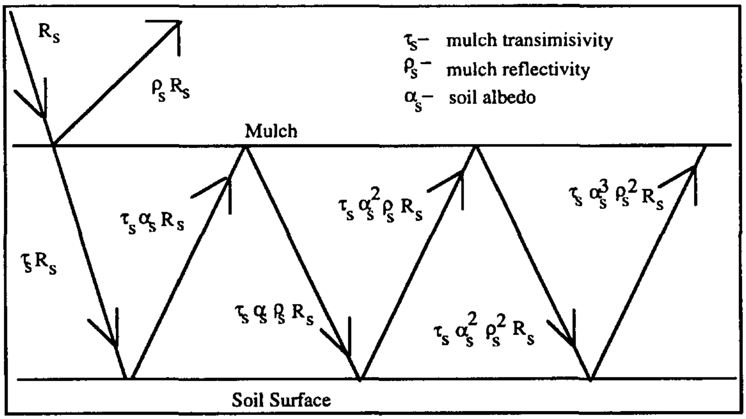

Fig. 1. Schematic of short wave radiation transfer inside the mulch.

Rearranging the terms on the right side of the equation results in the following equation:

$$\text{Term A} = (1 - a_s)\boldsymbol{R}_s\tau_s(1 + a_s\,\rho_s + a_s^2\,\rho_s^2 + a_s^3\,\rho_s^3 + a_s^4\,\rho_s^4 + \cdots)$$

where $(1 + a_s\,\rho_s + a_s^2\,\rho_s^2 + a_s^3\,\rho_s^4 + \cdots)$ equals $1/(1 - a_s\,\rho_s)$ mathematically. Therefore, Term A $= \boldsymbol{R}_s\tau_s(1 - a_s)/(1 - a_s\,\rho_s)$. Term B, C, and D are derived in the same manner as term A.

Heat exchanges between it and the mulch by convection from the mulch to the ambient air, and are determined by the temperature gradient. The sensible heat flux between the trapped air and the soil surface, $\boldsymbol{H}$, is calculated using the formula of Garzoli and Blackwell (1981).

$$\boldsymbol{H} = h_i(T_m - T) \tag{22}$$

where the temperature of the trapped air is assumed to be the same as the temperature of the mulch ($T_m$) because the air gap between the mulch and the soil surface is very thin, $h_i$ is the heat transfer coefficient (W m$^{-2}$ K$^{-1}$) inside the mulch.

The latent heat flux is given by:

$$\boldsymbol{\lambda E} = L(q_a - q_s)/(r_a + r_m) \tag{23}$$

where $r_m$ is the mulch resistance to evaporation (s m$^{-1}$). The material of mulch used for solarization in this study was polyethylene which does not transmit water (Mahrer, 1979; Waggoner et al., 1960). Therefore, $r_m$ was assumed to be infinite, and consequently $\boldsymbol{\lambda E}$ was zero.

The soil heat flux is determined as in the bare soil.

$$\boldsymbol{G} = \lambda(\delta T/\delta z) \tag{24}$$

where $\lambda$ is the same as in Eq. (1).

### 3.3. Mulch surface

The net radiation flux at the mulch surface is given by:

$$\begin{aligned}\boldsymbol{R}_{\mathrm{n}} = {} & \underbrace{\boldsymbol{R}_{\mathrm{s}}\left[(1-\rho_{\mathrm{s}})-\tau_{\mathrm{s}}(1-a_{\mathrm{s}}+\tau_{\mathrm{s}}a_{\mathrm{s}})/(1-\rho_{\mathrm{s}}a_{\mathrm{s}})\right]}_{\mathrm{A}} \\ & \underbrace{+\boldsymbol{R}_{\mathrm{a}}\left[(1-\rho_{\mathrm{l}})-\tau_{\mathrm{l}}(\tau_{\mathrm{l}}+\epsilon_{\mathrm{s}}(1-\tau_{\mathrm{l}}))/(1-\rho_{\mathrm{l}}+\rho_{\mathrm{l}}\epsilon_{\mathrm{s}})\right]}_{\mathrm{B}} \\ & \underbrace{-\epsilon_{\mathrm{m}}\sigma T_{\mathrm{m}}^4\left[2-(1-\epsilon_{\mathrm{s}})(1-\tau_{\mathrm{l}}-\rho_{\mathrm{l}})/(1-\rho_{\mathrm{l}}+\rho_{\mathrm{l}}\epsilon_{\mathrm{s}})\right]}_{\mathrm{C}} \\ & \underbrace{+\epsilon_{\mathrm{s}}\sigma T^4\left[1-(\tau_{\mathrm{l}}+\rho_{\mathrm{l}})/(1-\rho_{\mathrm{l}}+\rho_{\mathrm{l}}\epsilon_{\mathrm{s}})\right]}_{\mathrm{D}} \end{aligned} \tag{25}$$

The terms labeled A, B, C and D in Eq. (25) are the net short wave radiation, net long wave radiation from atmosphere, long wave radiation from the mulch and long wave radiation from the soil surface respectively. These terms are also affected by both mulch optical properties and soil properties and conditions. They are derived as described for term A in Eq. (21).

The sensible heat flux at the mulch surface consists of two parts: one due to the convection above the mulch, the other due to the convection below the mulch, and is calculated using the following equation:

$$\boldsymbol{H} = C_{\mathrm{p}}(T_{\mathrm{a}}-T_{\mathrm{m}})/r_{\mathrm{a}} + h_i(T-T_{\mathrm{m}}) \tag{26a}$$

where $r_{\mathrm{a}}$ is the same as in Eq. (9), $h_i$ is the same as in Eq. (22), the temperature of the air below the mulch is assumed to be the same as the soil surface temperature.

The sensible heat flux can also be calculated using the formula of Garzoli and Blackwell (1981):

$$\boldsymbol{H} = h_{\mathrm{o}}(T_{\mathrm{a}}-T_{\mathrm{m}}) + h_i(T-T_{\mathrm{m}}) \tag{26b}$$

where $h_{\mathrm{o}}$ is the heat transfer coefficient ($\mathrm{W\,m^{-2}\,K^{-1}}$) above the mulch, $h_i$ is the same as in Eq. (22).

The latent heat $\boldsymbol{\lambda E}$ equals zero based on the assumption given for Eq. (23). $\boldsymbol{G}$ also equals zero because here only the energy balance at the mulch surface is analyzed.

Eq. (1) is solved using Gaussian elimination methods (Remson et al., 1971). Eq. (1) can be written as a difference equation:

$$\frac{T_i^{n+1}-T_i^n}{\delta t} = \frac{D_{i-1}^{n+1}\left(T_i^{n+1}-T_{i-1}^{n+1}\right)-D_{i+1}^{n+1}\left(T_{i+1}^{n+1}-T_i^{n+1}\right)}{(\delta z)^2} \tag{27}$$

where $D$ is thermal diffusivity ($\mathrm{m^2\,s^{-1}}$) and $D=\lambda/C$, subscript $i$ is space step, and superscript $n$ is time step.

Eq. (27) can be rewritten as:

$$-D_{i-1}^{n+1}T_{i-1}^{n+1} + D_i^{n+1}T_i^{n+1} - D_{i+1}^{n+1}T_{i+1}^{n+1} = \left((\delta z)^2/\delta t\right)T_i^n \tag{28}$$

where $D_i^{n+1} = ((\delta z)^2/\delta t) + D_{i+1}^{n+1} + D_{i+1}^{n+1}$.

Eq. (28) can be solved using elimination methods when the boundary conditions are given.

Eq. (5) is solved using the Newton iteration method (Remson et al., 1971). Under steady state conditions it can be expressed as:

$$f(T) = \boldsymbol{R}_{\mathrm{n}} + \boldsymbol{H} + \boldsymbol{\lambda E} + \boldsymbol{G} = 0 \tag{29}$$

According to Newton's iterative technique, if $f(T) = 0$, then one can expand $f(T)$ in a Taylor series about $T^n$ retaining two terms, i.e.

$$f(T^{n+1}) = f(T^n) + f'(T^n)(T^{n+1} - T^n)$$

where $f'(T^n)$ is the derivative of the function $f(T^n)$ evaluated at $T^n$.

Then, with $f(T^{n+1}) = 0$

$$T^{n+1} = T^n - f(T^n)/f'(T^n) \tag{30}$$

## 4. Model validation

The Horticultural Crops Research Station (north latitude 35.00; west longitude 78.28; elevation 48.2 m) located near Clinton, NC, was the validation site. The topography in this Coastal Plain section of North Carolina is gently rolling. The soils are unconsolidated moderately fine to coarse textured Coastal Plain sediments. The soil is a well drained Nob–Norfolk loamy sand, with loamy sand A horizons. It has slopes ranging from 2 to 6 percent. The thickness of the loamy sand A is variable, from less than 15 to 50 cm. The B horizons are yellowish brown sand clay loam extending to depths of more than 150 cm.

To run the model, two input files are required, one for the inputs of soil physical properties, mulch optical properties, initial values of soil temperature and moisture, the surface roughness length, and the thickness of each soil sublayer; the other for the inputs of atmospheric data including hourly measurements of global radiation, air temperature, dewpoint, wind speed and rainfall.

The soil parameter values and the mulch optical properties are shown in Table 1. The soil bulk density, soil porosity, saturated and residual soil water contents are from Williams et al. (1990). The fractions of clay, organic matter and quartz are from Williams et al. (1990), North Carolina Agricultural Experiment Station (1977), and Hendricks and Fry (1986). These values were measured or derived for the soil type at the Horticultural Crops Research Station. The shape factors of air, clay, organic matter, quartz and water, Van Genuchten parameters and Ten Berge parameters and saturated hydraulic conductivity are from Ten Berge (1990). The values of these parameters in this study were chosen based on the saturated and residual soil water contents as well as the description of soil type. The initial soil temperature of the surface and bottom layer are 42 and 8°C for the bare soil, 48 and 8°C for the mulched soil, respectively. These values change from location to location, especially from latitude to latitude. If they are not given accurately, the model needs more time steps or a longer time period to converge on the best estimate. In this study, they were chosen based on the measured values and obtaining the shortest time period for the model to converge on the best estimate (the smallest absolute difference between the first measured and estimated values). The initial soil moisture values for the top 10 sublayers are 0.17 and increased

Table 1
Soil, mulch and other constant parameters and their symbol, value and units

| Parameters | Symbol | Value | Unit |
|---|---|---|---|
| *1. Soil parameters* | | | |
| soil bulk density | $BD$ | 1.710 | $1000\ kg\,m^{-3}$ |
| saturated soil moisture | $\theta_s$ | 0.36 | $m^3\,m^{-3}$ |
| residual soil moisture | $\theta_r$ | 0.06 | $m^3\,m^{-3}$ |
| soil porosity | $P_o$ | 0.36 | dimensionless |
| fraction of clay | $F_c$ | 0.19 | $m^3\,m^{-3}$ |
| fraction of organic matter | $F_o$ | 0.03 | $m^3\,m^{-3}$ |
| fraction of quartz | $F_q$ | 0.42 | $m^3\,m^{-3}$ |
| shape factor of air | $SF_a$ | 0.200 | dimensionless |
| shape factor of clay | $SF_c$ | 0.010 | dimensionless |
| shape factor of organic matter | $SF_o$ | 0.500 | dimensionless |
| shape factor of quartz | $SF_q$ | 0.140 | dimensionless |
| shape factor of water | $SF_w$ | 0.140 | dimensionless |
| saturated hydraulic conductivity | $K_s$ | $6.380\times10^{-6}$ | $kg\,m^{-1}\,s^{-1}\,Pa^{-1}$ |
| *2. Optical properties of mulch* | | | |
| transmissivity of mulch to solar radiation | $\tau_s$ | 0.89 | dimensionless |
| transmissivity of mulch to long wave radiation | $\tau_l$ | 0.80 | dimensionless |
| reflectivity of mulch to solar radiation | $\rho_s$ | 0.06 | dimensionless |
| reflectivity of mulch to long wave radiation | $\rho_l$ | 0.16 | dimensionless |
| *3. Others* | | | |
| Van Genuchten parameter ($\alpha$) | Van1 | $2.761\times10^{-4}$ | $Pa^{-1}$ |
| Van Genuchten parameter ($n$) | Van2 | 3.0224 | dimensionless |
| hydraulic scale length | scale | 2.0 | dimensionless |
| vapor diffusion enhancement factor ($\beta$) | Beta | 1.25 | dimensionless |
| gravimetric moisture at soil relative humidity of 80% | $w_{80}$ | 0.20 | kg water/kg soil |
| surface roughness length for the bare soil | $z_o$ | 0.001 | m |
| surface roughness length for the mulched soil | $z_o$ | 0.0001 | m |

to 0.36 linearly with depth for the rest of the sublayers, where 0.36 is the saturated soil moisture. These initial values were chosen based on Neutron Probe readings in sweet potato fields near the solarized site in the summer of 1990.

The transmissivities of the mulch to short and long wave radiation are from Godbey et al. (1979), and the absorptivities of the mulch to short and long wave radiation are from Katan and DeVay (1991). Then the reflectivities of the mulch to short and long wave radiation are determined by subtracting corresponding transmissivity and absorptivity from unity. The values of these parameters were measured or derived for new polyethylene (PE) in Godbey et al. (1979) and Katan and DeVay (1991). The mulch material used in our solarization experiments was also new polyethylene, and was installed in the experimental field on June 6, 1990.

The surface resistance ($r_s$) in Eq. (14) is related to the length of the diffusion pathway through the soil (Stewart, 1984). Four different kinds of methods calculating $r_s$ have been reported. One is the theoretical analysis method used by Fuchs and Tanner (1967), in which $r_s$ is given by $r_s = (0.622L\rho/P)(e_s - e_s^o)/E$, where $L$ is latent heat of vaporization of water, $\rho$ is air density, $P$ is air pressure, $e_s$ is water pressure at the surface $e_s^o$ is saturated water vapor pressure corresponding to the soil surface temperature, $E$ is evaporation. However, Fuchs and Tanner (1967) failed to describe correctly the transfer processes through the dry upper layer of the soil using the method.

The second method is that of Novak and Black (1985) and Hares and Novak (1992a,b) in which $r_s$ was determined by trial and error until the measured and calculated daily average values of latent heat flux agreed to within 1 $W m^{-2}$ or according to their measured soil water contents and measured soil water-retention curves. The value of $r_s$ in their study was set to a constant for periods of interest. This method is not practical because $r_s$ could not be a constant for long time period and the measured soil water contents and measured water-retention curves are not available in most regions. Hares and Novak (1992b) found that considerable difference existed between predicted bare-plot values of latent heat flux and measurements.

The third method is that of Pikul (1991) in which $r_s$ is calculated by the following equation: $r_s = \rho C_p D_q \gamma F$, where $\rho C_p$ is the volumetric heat capacity of air, $D_q$ is the vapor pressure deficit, $\gamma$ is the psychrometric constant, $F$ is the experimentally determined factor given as a function of accumulated net radiation from the last rain. Therefore, $F$ will change from site to site and from time to time.

The forth method is the simple relationship of $r_s$ to soil water content, $\theta$, which was developed by Sun (1982) and Camillo and Gurney (1986). According to Camillo and Gurney (1986), $r_s$ can be expressed as a linear function of the difference between saturated and actual soil water content, i.e., $r_s = A + B(\theta_s - \theta)$, where $A$ and $B$ are regression coefficients which can be determined if evaporation measurements are available.

In this study, when $r_s$ was determined by the equation of Camillo and Gurney (1986), good agreement between the calculated and measured soil temperatures were obtained, because

1. the saturated and residual water contents (0.36 and 0.06 respectively) in our study are very close to those in Camillo and Gurney (1986) which are 0.39 and 0.05 respectively, and
2. the range from the residual water content to the saturated water content for the soil in Camillo and Gurney (1986) is a little wider than the range in this study.

When $r_s$ was determined by $E = (q_a - q_s)/(r_a + r_s)$, the agreemnet between the calculated and measured soil temperatures was a little better. Therefore, it is the final method for $r_s$ in this study.

The heat transfer coefficients in Eqs. (22), (26a) and (26b) are the same as in Garzoli and Blackwell (1981), i.e. $h_i = 7.2$ ($W m^{-2} K^{-1}$), and $h_o = (7.2 + 3.8u)$ ($W m^{-2} K^{-1}$). These two coefficients were derived for heat exchange from a single skin plastic greenhouse from data obtained in 18 experiments by Garzoli and Blackwell (1981). The combinations of temperature and relative humidity in the experiments were varied. Each of the combinations represented one climatic condition. Therefore, it is anticipated that the values may be used for different applications. Using the coefficients, Garzoli and Blackwell (1981) obtained a good agreement between the calculated and measured rate of heat transfer from a single skin plastic greenhouse. It was found in this study that little difference exists between the estimated soil temperatures using Eqs. (26a) and (26b) in the model for both the mulched and bare soil cases.

The atmospheric data were collected by an automated weather station consisting of a data acquisition system (DAS) and the environmental parameter sensors. The DAS is composed of a DC112 modem and CR-10 measurement and control module, both by Campbell Scientific, Inc, Logan, UT. The DAS stores data every hour. The current

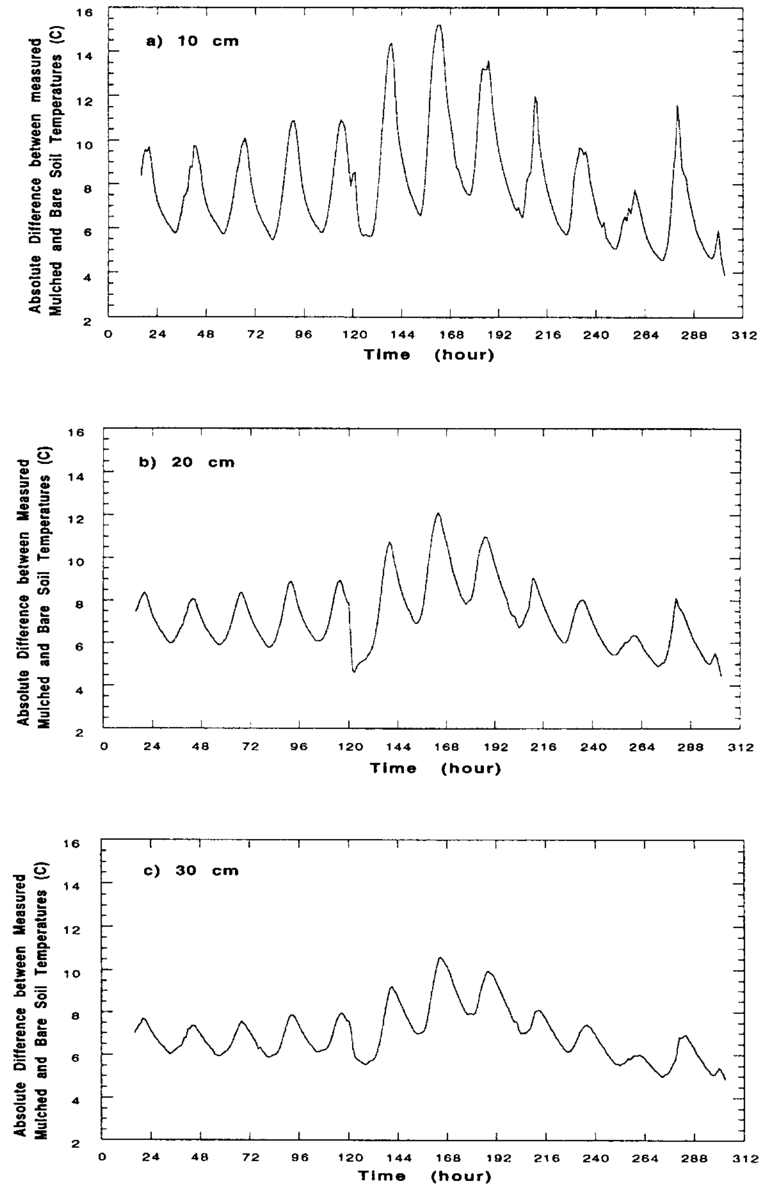


Fig. 2. Comparisons between the measured bare and measured mulched soil temperatures at the depths of (a) 10 cm, (b) 20 cm, and (c) 30 cm (July 6–18, 1990, Clinton, NC).

dry-bulb temperature, dewpoint, relative humidity, and rainfall of the previous hour are recorded at the top of the hour. The total solar radiation and wind speed are sampled every fifteen seconds, and then averaged for the hour readings. The dry-bulb tempera-

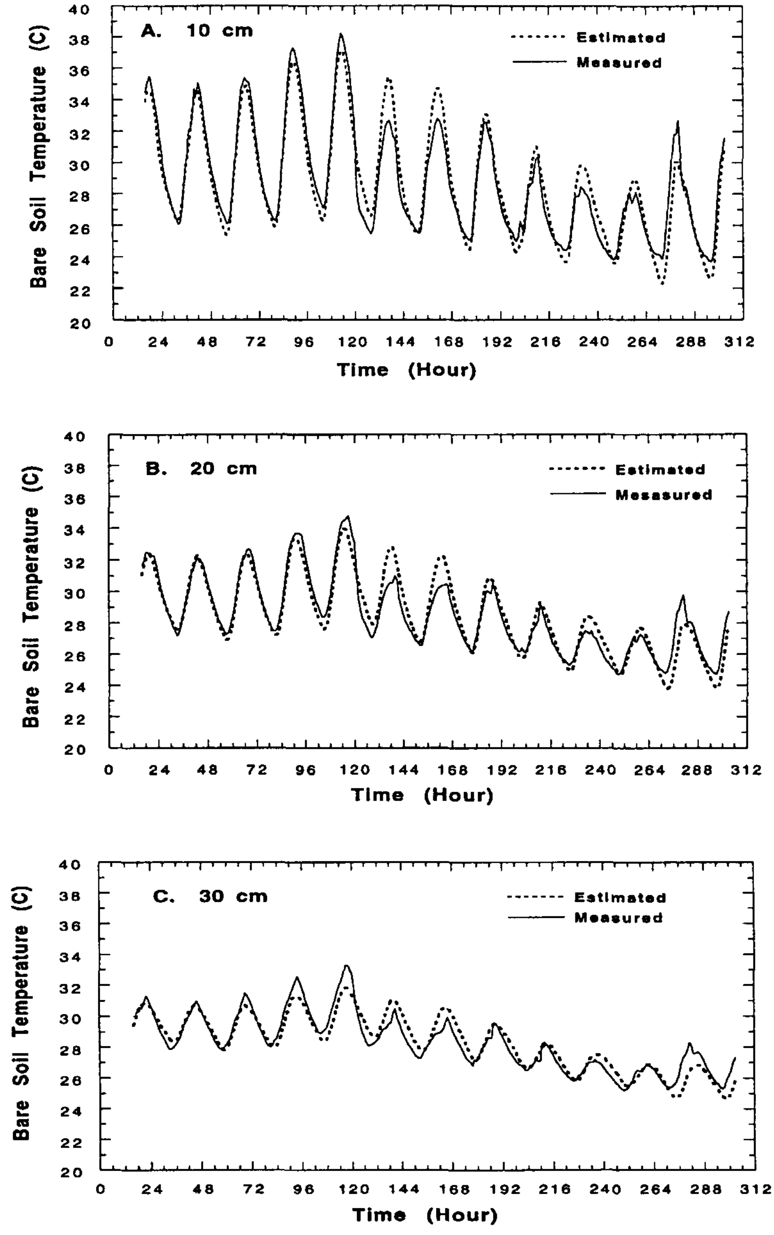


Fig. 3. Comparisons between the measured and estimated bare soil temperatures at the depths of (a) 10 cm, (b) 20 cm and (c) 30 cm (July 6–18, 1990, Clinton, NC).

ture and relative humidity are measured with a Vaisala (Helsinki, Finland) HMP-35C probe. Rainfall is measured by a model 1790 tipping bucket rain gage by Heath Company, Benton Harbor, MI. Total solar radiation is sampled by a model 8-48 pyranometer from Eppley Laboratories, Newport, RI. Wind speed is measured with a Climatronics Inc. (Bohemia, NY) model 100108 Mark 3 wind sensor crossarm. Consid-

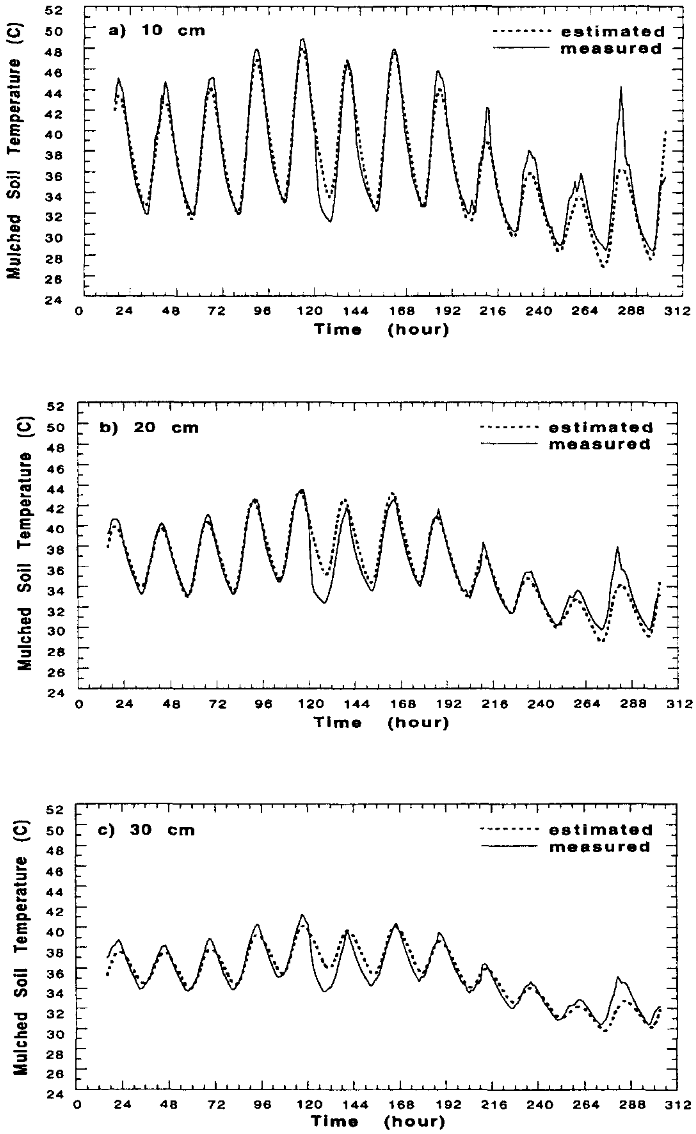


Fig. 4. Comparisons between the measured and estimated mulched soil temperatures at the depths of (a) 10 cm, (b) 20 cm and (c) 30 cm (July 6–18, 1990, Clinton, NC).

ering the development of this kind of automated weather station, hourly measurements of these weather elements are becoming readily available. The time step, $t$, can be any value between 0 and 3600 s (300 s was used here), even though input weather data for the model are hourly values. The required meteorological data at each time step are interpolated from the data of the previous hour and current hour. Global radiation, air temperature, and dewpoint temperature are determined as linear functions of time. Rainfall was evenly distributed over time and wind speed was assumed constant.

The mulched and bare soil temperature during June, July and August of 1990 and 1991 were monitored at the top of the hour with copper-constantan thermocouples recorded by a Campbell Scientific, Inc. CR21X micrologger. The sensors were buried in soil at 10, 20 and 30 cm depths in the field where solarization was carried out.

## 5. Results and discussion

Hourly soil temperature measurements for July 6–18, 1990, were used for validation. Unfortunately, additional testing was not possible due to lightning damage to the automated weather station early in the summer of 1991. During the period of July 6–18, 1990, varying weather conditions existed. July 6–10, 12 and 13 were clear days. July 11, 14–17 were rainy days. It rained almost the whole day on July 11, and 57.0 mm of

Table 2
Percentages of absolute differences less than 1C and 2C and relative differences less than 5% and 10%, the ranges of absolute differences, and the maximum relative differences between estimated and measured soil temperatures at three depths for bare and mulched soil

| Soil type | Soil depth | Percentage of absolute difference | | |
|---|---|---|---|---|
| | (cm) | < 1C | < 2C | Range (C) |
| Bare | 10 | 70% | 94% | −3.3– +2.8 |
| | 20 | 83% | 98% | −2.4– +2.2 |
| | 30 | 86% | 100% | −1.9– +1.4 |
| Mulched | 10 | 60% | 89% | −8.2– +4.4 |
| | 20 | 80% | 95% | −4.0– +5.1 |
| | 30 | 78% | 95% | −3.1– +3.1 |
| **Soil type** | **Soil depth** | **Percentage of relative difference** | | |
| | (cm) | < 5% | < 10% | Maximum |
| Bare | 10 | 85% | 99% | 11% |
| | 20 | 93% | 100% | 8% |
| | 30 | 96% | 100% | 7% |
| Mulched | 10 | 88% | 97% | 19% |
| | 20 | 92% | 98% | 15% |
| | 30 | 94% | 100% | 9% |

Note: Absolute difference = estimated − measured. Relative difference = 100(absolute difference/measured). %s of absolute (relative) differences less than the given criteria = 100 times the ratio of the number of absolute (relative) differences less than the given criteria to the total number of absolute (relative) differences.

rainfall were measured. On July 14, 15, 16, and 17, 6.0, 8.5, 0.5, and 3.0 mm of rainfall were measured, respectively. A significant decrease in air temperature (8.2°C in 1 h) was recorded around noon on July 17.

Outputs of the model include energy fluxes, soil temperature and moisture at different depths, evaporation from bare soil, Bowen ratio, aerodynamic resistance, soil heat capacity, thermal conductivity, and hydraulic conductivity. However, no actual measurements of evaporation, Bowen ratio, energy fluxes, soil moisture, aerodynamic resistance, soil heat capacity, thermal conductivity, and hydraulic conductivity are available for this analysis. These outputs were compared with published data, and good agreement existed (data not shown). The analysis in the following section focuses on soil temperature only.

### *5.1. Mulch effect on soil temperature*

The temperature in mulched soil was much higher than that in bare soil during period (Fig. 2). The differences between mulched and bare soil temperatures changed diurnally, and changed with soil depth. The differences were larger during daylight than at night, and larger near the surface than at deeper depth. The mean differences between mulched

Table 3
Hourly values of solar radiation (W m$^{-2}$), air temperature (°C), and wind speed (m s$^{-1}$) for July 16 and 17, 1990

| Hour | July 16 | | | July 17 | | |
|---|---|---|---|---|---|---|
| | Solar radiation | Air temperature | Wind speed | Solar radiation | Air temperature | Wind speed |
| 1 | 0.0 | 25.4 | 0.6 | 0.0 | 24.1 | 0.0 |
| 2 | 0.0 | 25.2 | 0.2 | 0.0 | 23.3 | 0.0 |
| 3 | 0.0 | 25.6 | 0.2 | 0.0 | 23.7 | 0.0 |
| 4 | 1.0 | 25.6 | 0.1 | 0.0 | 23.5 | 0.0 |
| 5 | 15.0 | 25.3 | 0.7 | 62.0 | 23.4 | 0.0 |
| 6 | 63.0 | 25.0 | 0.1 | 206.0 | 23.9 | 0.0 |
| 7 | 206.0 | 25.5 | 1.2 | 297.0 | 26.9 | 0.1 |
| 8 | 249.0 | 25.7 | 0.5 | 399.0 | 27.2 | 0.1 |
| 9 | 320.0 | 28.3 | 1.2 | 512.0 | 28.5 | 0.0 |
| 10 | 238.0 | 26.7 | 2.4 | 615.0 | 28.8 | 0.1 |
| 11 | 244.0 | 27.1 | 0.8 | 538.0 | 29.8 | 0.1 |
| 12 | 359.0 | 28.8 | 0.9 | 840.0 | 31.5 | 0.6 |
| 13 | 165.0 | 25.3 | 1.8 | 318.0 | 23.3 | 4.2 |
| 14 | 331.0 | 25.6 | 1.1 | 147.0 | 23.5 | 2.5 |
| 15 | 402.0 | 28.8 | 2.1 | 258.0 | 25.0 | 1.3 |
| 16 | 147.0 | 26.8 | 2.4 | 257.0 | 25.7 | 1.4 |
| 17 | 91.0 | 27.0 | 2.1 | 59.0 | 25.5 | 0.3 |
| 18 | 31.0 | 26.8 | 0.6 | 37.0 | 25.0 | 2.3 |
| 19 | 0.0 | 23.7 | 1.0 | 0.0 | 25.2 | 1.5 |
| 20 | 0.0 | 24.1 | 1.4 | 0.0 | 23.8 | 0.6 |
| 21 | 0.0 | 23.6 | 1.0 | 0.0 | 23.7 | 0.0 |
| 22 | 0.0 | 20.3 | 1.1 | 0.0 | 23.8 | 0.0 |
| 23 | 0.0 | 23.8 | 0.6 | 0.0 | 23.7 | 0.0 |
| 24 | 0.0 | 24.0 | 0.0 | 0.0 | 23.4 | 0.0 |

and bare soil temperatures at 10, 20, and 30 cm depth were 7.41, 7.28 and 6.99 (°C) respectively. In other words, the average temperatures at 10, 20 and 30 cm depth in mulched soil were 7.41, 7.28 and 6.99 (°C) respectively higher than those in bare soil. The maximum differences between mulched and bare soil temperatures for the three depths were 15.23, 12.12 and 10.60 (°C), and occurred on July 12, 6:00–7:00 PM (hour 162–163 in Fig. 2), 8:00 PM (hour 164 in Fig. 2) and 9:00 PM (hour 165 in Fig. 2) respectively. However the maximum temperatures in the mulched and bare soils occurred on July 10 (hour 97–120 in Fig. 3 and Fig. 4). Comparison between the measurements in mulched and bare soils (Fig. 3 and Fig. 4) showed:

1. Temperatures of both bare and mulched soil at the same depth changed synchronously with time.
2. Both had a significant diurnal cycle.
3. The diurnal variation amplitude of temperature in mulched soil was relatively larger than that in bare soil.

This is different from the report in Katan and DeVay (1991).

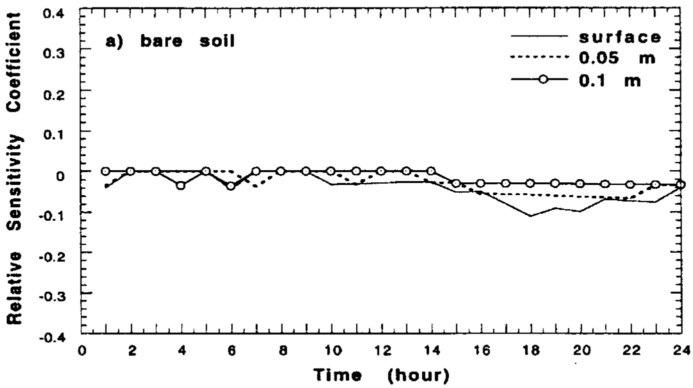


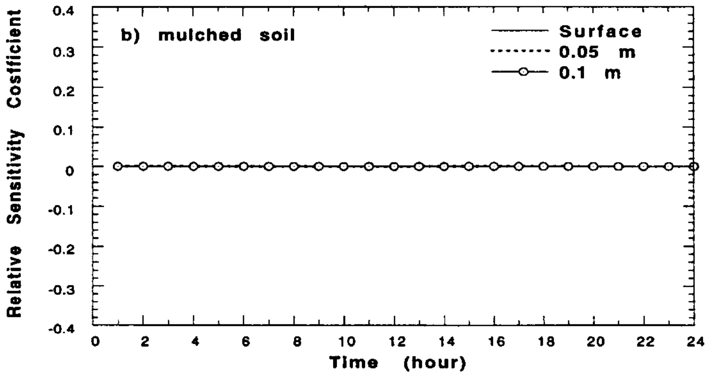


Fig. 5. Relative sensitivity of the model to 10% change in surface roughness length ($z_0$) in the cases of (a) bare soil, and (b) mulched soil.

### 5.2. Soil temperature simulations

The estimates of both bare and mulched soil temperature at 10, 20 and 30 cm depth were compared with the corresponding measured values by examining diurnal variation, difference and correlation. In the bare soil case, the diurnal variations of estimated and measured bare soil temperatures at the three depths were synchronous, and the amplitudes of diurnal variations of both estimated and measured soil temperatures decreased with soil depth (Fig. 3(a)–(c)). The correlation between estimated and measured temperatures produced $R$-square values of 0.89, 0.87 and 0.82 for the three depths, respectively. The range of absolute differences between estimated and measured bare soil temperatures at 10, 20 and 30 cm depth were −3.30 to +2.80°C (Fig. 3(a)), −2.40 to +2.20°C (Fig. 3(b)) and −1.90 to +1.40°C (Fig. 3(c)), respectively, and the largest differences occurred at shallow depths (Fig. 3(a)). The percentages of the absolute differences less than 1.0°C or 2.0°C between the estimated and measured bare soil

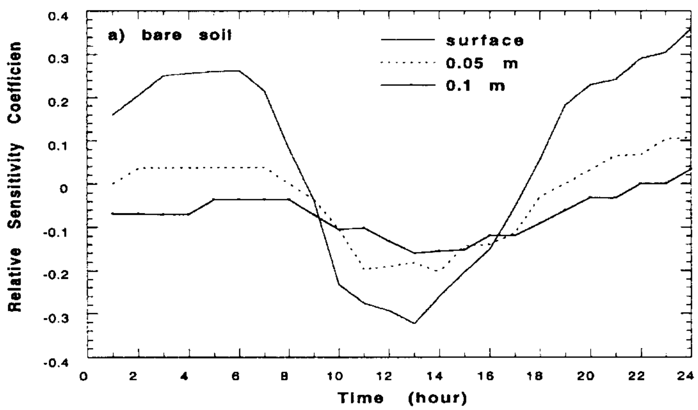


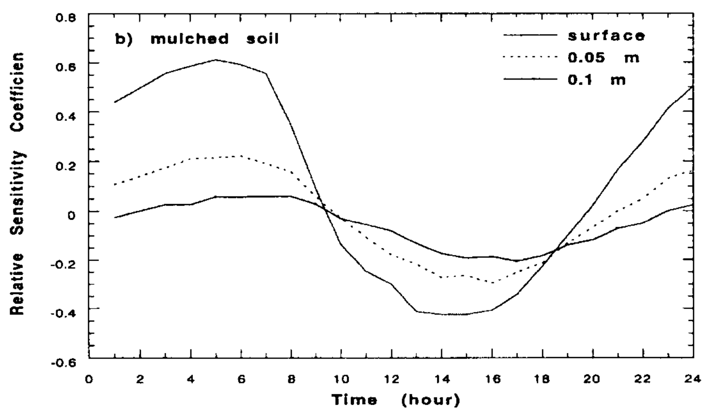


Fig. 6. Relative sensitivity of the model to 10% change in soil bulk density (BD) in (a) bare soil, and (b) mulched soil.

temperatures were 70, 83 and 86, and 94, 98 and 100 at 10, 20, and 30 cm depths, respectively (Table 2).

In the mulched soil case, the diurnal variation of the estimated and the measured soil temperatures at the three depths occurred synchronously, and amplitudes of diurnal variations of both estimated and measured soil temperatures decreased with soil depth (Fig. 4(a)–(c)). The correlation between estimated and measured temperatures yielded $R$-square values of 0.93, 0.91 and 0.88 for the three depths, respectively, and were higher than those for bare soil. The absolute differences between the estimated and the measured values at 10, 20 and 30 cm depth range from −8.20 to +4.40°C (Fig. 4(a)), −4.00 to +5.10°C (Fig. 4(b)), and −3.10 to +3.10°C (Fig. 4(c)), respectively. These absolute differences were larger than those for bare soil. The percentages of the absolute differences less than 1.0°C or 2°C between the estimated and measured soil temperatures were 60, 80 and 78, and 89, 95 and 95, at 10, 20, and 30 cm depth, respectively (Table 2).

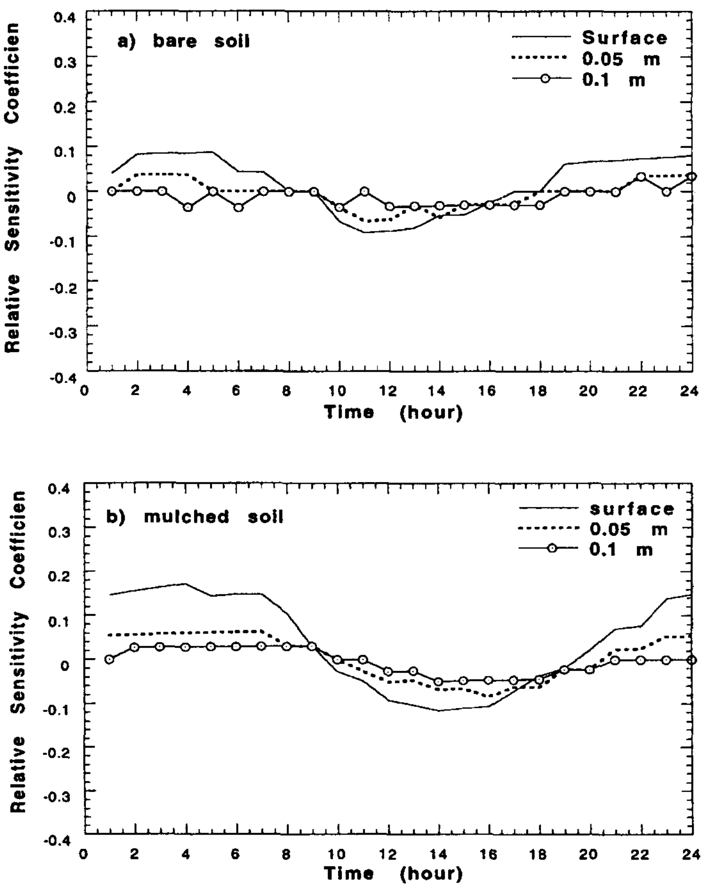


Fig. 7. Relative sensitivity of the model to 10% change in clay fraction ($F_c$) in (a) bare soil, and (b) mulched soil.

Both $R$-square values and absolute differences decreased with depth in both the bare and mulched soil cases. The model estimated soil temperatures accurately on both clear and rainy days in both cases except July 17 (hour 264 to 288 on Figs. 3 and 4) when the largest differences occurred in both cases. The model underestimated the mulched soil by 8.20°C (Fig. 4(a)) and the bare soil by 3.30°C (Fig. 3(a)) on that day. However, the largest difference in bare soil occurred one hour (1700) later than in mulched soil (1600) (data not shown). July 16 was cloudy, and 0.5 mm of rainfall was recorded, but the morning of July 17 was very clear, as indicated by solar radiation (Table 3). A severe storm occurred about noon causing the air temperature to drop by 8.20°C, and the global solar radiation to drop from 840 to 318 W m$^{-2}$ within one hour. This suggests that the model is not sensitive enough to large, rapid changes of the air temperature and solar radiation. This might be due to the interpolations of global radiation and air temperature for each time step. That global radiation and air temperature were interpolated linearly

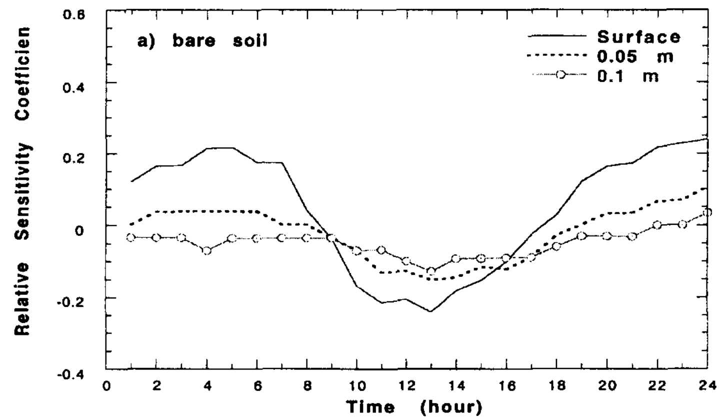


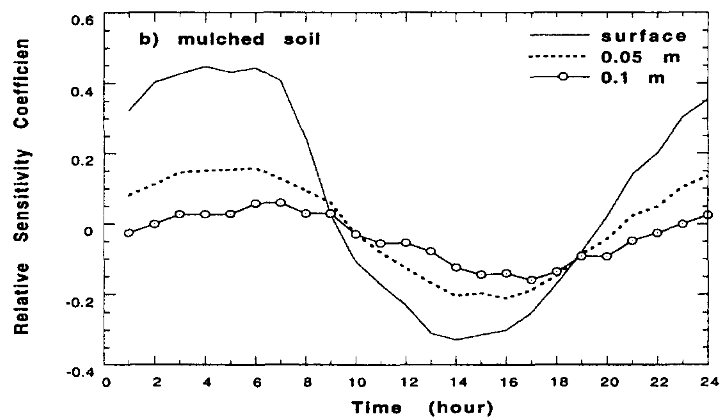


Fig. 8. Relative sensitivity of the model to 10% change in quartz fraction ($F_q$) in (a) bare soil, and (b) mulched soil.

with time would usually underestimate global radiation and air temperature during daylight and overestimate air temperature at night. This could lead the model to underestimate soil temperature during daylight and overestimate soil temperatures at night. This could have a greater effect during daylight, because solar radiation strongly affects the surface energy balance during daylight.

### 5.3. Model sensitivity

Sensitivity analyses were performed for both simulations of bare and mulched soils. The effects of changes in all the constant input parameters in Table 1 were investigated. The relative sensitivity coefficients, $\sigma(Y/P) = (Y(P) - Y(P + \Delta P))/Y(P)) \times (P/\Delta P)$, were used to describe the sensitivity of the model, where $Y$ represents soil temperature, and $P$ represents each parameter. Therefore, the relative sensitivity coeffi-

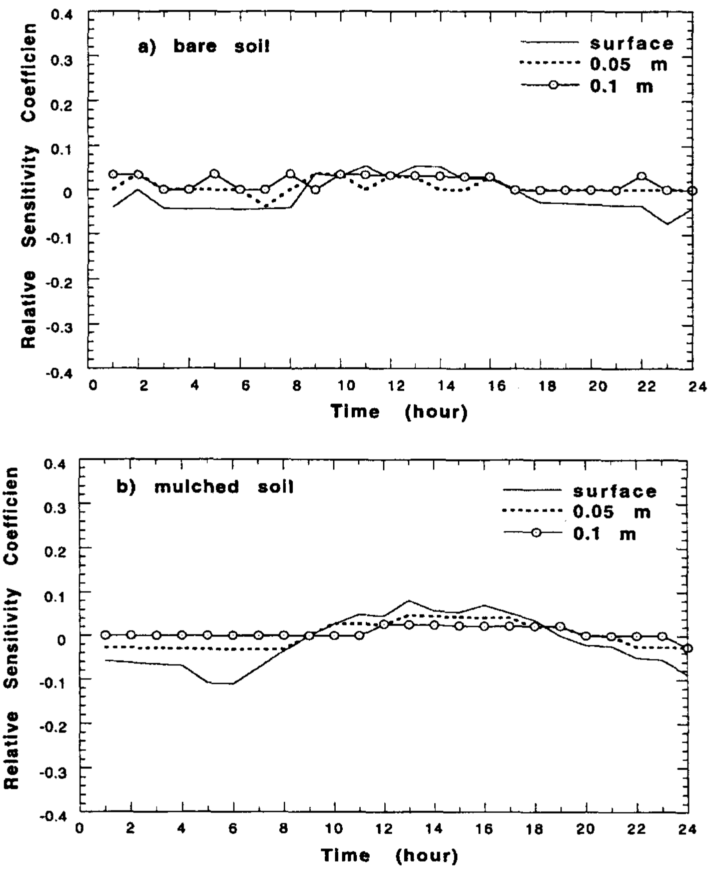


Fig. 9. Relative sensitivity of the model to 10% change in quartz shape factor ($SF_q$) in (a) bare soil, and (b) mulched soil.

cient indicates the relative soil temperature change due to the relative change of each parameter. For each parameter, a simulation was run for a period of 56 h. Data from the last 24 h were analyzed to reduce the effects of initial conditions. The relative sensitivity coefficients for the surface, 0.05 and 0.1 m depth were calculated by increasing each parameter by 10% while holding all other parameters constant. Here a relative sensitivity coefficient of 0.1 or greater was designated as sensitive. This means that a 10% change in the parameter creates a 10% or greater change in soil temperature prediction.

The model was sensitive to surface roughness length in the bare soil case (Fig. 5(a)). The relative sensitivity coefficients at surface layer were larger compared with the relative sensitivity coefficients at lower depths. However, the model was not sensitive to the surface roughness length in the mulched soil case (Fig. 5b). The reason is that evaporation was assumed zero due to the mulch. The model was very sensitive to soil bulk density (Fig. 6), clay fraction (Fig. 7) and quartz fraction (Fig. 8) in both bare and

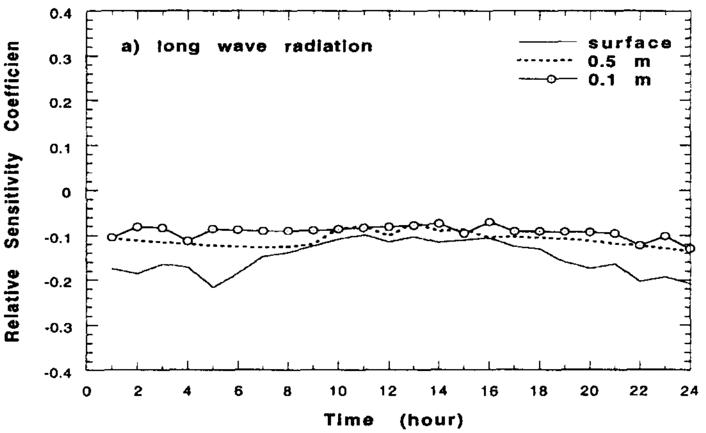


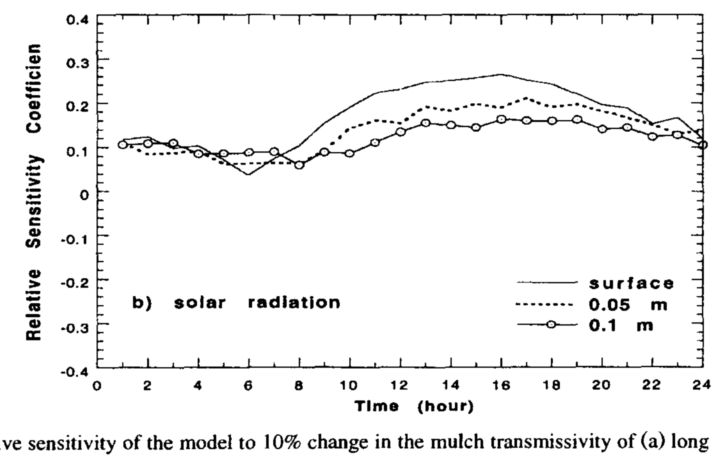


Fig. 10. Relative sensitivity of the model to 10% change in the mulch transmissivity of (a) long wave radiation ($\tau_l$), and (b) solar radiation ($\tau_s$).

mulched soils. The relative sensitivity coefficients were positive at night and negative during day time. This suggests that increasing soil bulk density, clay and quartz fractions could increase soil heat capacity which decreases the amplitude of the diurnal variation of soil temperature. The relative sensitivity coefficients of the three parameters were larger at the surface than at other depths in both bare and mulched soils. The relative sensitivity coefficients for soil bulk density and quartz fraction were larger in mulched soil (Fig. 6(b) and Fig. 8(b)) than in bare soil (Fig. 6(a) and Fig. 8(a)), indicating that the model responded more strongly to the changes in these two parameters in mulched soil than in bare soil. However, the magnitude of the difference of relative sensitivity coefficients for clay fraction between mulched and bare soil (Fig. 7(a) and (b)) were not as large as for the soil bulk density or quartz fraction. The model also was sensitive to quartz shape factor in both bare and mulched soils (Fig. 9). However, except for several exceptions in bare soil, the effect was reversed, indicated by positive values during day time and negative values at night time. This indicated that an increase in the quartz shape factor increased the amplitude of the diurnal variation of soil temperature.

The model was sensitive to mulch transmissivity of solar and long wave radiation (Fig. 10). The relative sensitivity coefficients were negative for mulch transmissivity to long wave radiation (Fig. 10(a)) and positive for mulch transmissivity to solar radiation (Fig. 10(b)). An increase in mulch transmissivity to solar radiation could increase the soil temperature estimate, but an increase in mulch transmissivity to long wave radiation could decrease soil temperature estimate. This indicates that the long wave radiation from soil surface is greater than that from the atmosphere, especially at night time, shown by larger values at night time (Fig. 10(a)). The relative sensitivity coefficients of the model to mulch reflectivities of solar and long wave radiation were less than 0.1 (data not shown), indicating that the model was not sensitive to these parameters. However, there was a slight positive trend of the relative sensitivity coefficients of the model mulch reflectivities to long wave radiation, and a negative trend of the relative sensitivity coefficients of the model mulch reflectivities to solar radiation. This could indicate that an increase in mulch reflectivity of solar radiation could decrease the soil temperature estimate, and an increase in mulch reflectivity of long wave radiation could increase the soil temperature estimate.

The model was not sensitive to the other parameters, including saturated and residual soil moisture, fraction of organic matter, shape factors of air, clay, organic matter and water, Van Genuchten and Ten Berge parameters (data not shown). However, the variation of the relative sensitivity coefficients in all cases decreased with soil depth, and could suggest that the model was responding to each parameter more strongly at the surface.

## 6. Conclusion

The effect of mulch on increasing soil temperature is determined by the optical properties of mulch and the physical properties of soil as well as the weather conditions. During the solarization period of 1990 at Clinton, NC, temperature in mulched soil was much higher than that in bare soil. The differences between mulched and bare soil temperatures changed diurnally, and changed with soil depth. They were larger during daylight than at night, larger at shallow depth than at deep depth. A model in which the optical properties of mulch, the physical properties of soil conditions, as well as the atmospheric conditions are considered has been developed in this study to investigate the effect. The model is physically based. No particular assumptions were made based on local conditions. Therefore, the model will work very well under various climate, soil and mulch conditions, if the required inputs, i.e. soil parameters, surface roughness length, and optical properties of mulch are measured or estimated correctly. The model accurately simulated the soil temperatures for both bare and mulched soils on both clear and rainy days during July 6–18, 1990 at Clinton, NC. However, the model did not work well when large, rapid changes of the air temperature and solar radiation occurred on July 17. If the model is used to investigate the effect of mulch on increasing soil temperature in all seasons, further tests and validation should be carried out for soil temperature in spring and fall seasons during which large and rapid weather changes occur more frequently, and for the other estimated parameters, such as energy fluxes and soil water content. The outputs of the model, including not only the estimated soil temperature, but also the estimated energy fluxes, evaporation, soil water content, and soil heat capacity, etc., can provide valuable information for numerous practical applications including determination of sowing date, application of fertilizer, and the solarization application described herein.

## Acknowledgements

The authors express their sincere appreciation to Dr. H.F.M. Ten Berge for providing the FORTRAN utility library and reference manual, and Dr. J.R. Kiniry for providing the EPIC soil data base. Authors also express appreciation to Y. Mahrer and J. Katan for providing a copy of their soil temperature model used in preliminary analysis, and Dr. J.H. Young for reviewing and useful suggestions that greatly improved this manuscript. Finally, authors thank the regional editor and the reviewers for their comments and suggestions.

## References

Camillo, P.J. and Gurney, R.J., 1986. A resistance parameter for bare-soil evaporation models. Soil Sci., 141(2): 95–105.

Cenis, J.L., 1989. Temperature evaluation in solarized soils by Fourier analysis. Phytopathology, 79: 506–510.

Chen, Y.S. and Jiang, R.B., 1989. Meteorology (in Chinese). Meteorological Publisher, Beijing.

De Vries, D.A., 1963. Thermal properties of soils. In: W.R. Van Wijk (Editor), Physics of Plant Environment. North-Holland, Amsterdam, pp. 210–235.

Fuchs, M. and Tanner, C.B., 1967. Evaporation from a drying soil. J. Appl. Meteorol., 6: 852–857.

Garzoli, K.V. and Blackwell, J., 1981. An analysis of the nocturnal heat loss from a single skin plastic greenhouse. J. Agric. Eng. Res., 26: 203–214.

Godbey, L.C., Bond, T.E. and Zornig, H.F., 1979. Transmission of solar and long wavelength energy by materials used as covers for solar collectors and greenhouses. Trans. ASAE, 22(5): 1137–1144.

Hares, M.A. and Novak, M.D., 1992a. Simulation of surface energy balance and soil temperature under strip tillage: I. Model description. Soil Sci. Soc. Am. J., 56: 22–29.

Hares, M.A. and Novak, M.D., 1992b. Simulation of surface energy balance and soil temperature under strip tillage: II. Field test. Soil Sci. Soc. Am. J., 56: 29–36.

Hendricks, S.B. and Fry, W.H., 1986. The results of X-ray and microscopical examinations of soil colloids. In: J.A. Kittrick (Editor), Soil Mineral Weathering. Van Nostrand Reinhold, New York, pp. 22–23.

Horton, R. and Chung, S., 1991. Soil heat flow. In: J. Hanks and J.T. Ritchie (Editors), Modeling Plant and Soil Systems. American Society of Agronomy, Inc., Madison, WI, pp. 397–438.

Katan, J. and DeVay, E., 1991. Solarization. CRC Press, Inc., Boca Raton, FL.

Mahrer, Y., 1979. Prediction of soil temperature of soil mulched with transparent polyethylene. J. Appl. Meteorol., 18: 1263–1267.

Mahrer, Y. and Katan, J., 1981. Spatial soil temperature regime under transparent polyethylene mulch: Numerical and experimental studies. Soil Sci., 131: 82–87.

Murray, F.M., 1967. On the computation of saturation vapor pressure. J. Appl. Meteorol. 6: 203–205.

North Carolina Agricultural Experiment Station, North Carolina Department of Agriculture, USDA, 1977. Soils of the horticultural crops research station, Clinton, NC, their technical and useability classification. North Carolina Agricultural Experiment Station, Raleigh, NC.

Novak, M.D. and Black, T.A., 1985. Theoretical Determination of the Surface Energy Balance and Thermal Regimes of Bare Soils. Boundary-Layer Meteorol., 33: 313–333.

Pikul, J.L., 1991. Estimating soil surface temperature from meteorological data. Soil Sci., 151(3): 187–194.

Remson, I., Hornberger, G.M. and Molz, F.J., 1971. Numerical methods in subsurface hydrology. John Wiley and Sons, Inc., New York, pp. 63–70 and 164–171.

Ristaino, J.B., Perry, K.B. and Lumsden, R.D., 1991. Effect of solarization and *Gliocladium virens* on *Sclerotium rolfsii*, soil microbiota, and the incidence of southern blight of tomato. Phytopathology, 81: 1117–1124.

Stewart, J.B., 1984. Measurement and prediction of evaporation from forested and agricultural catchments. In: M.L. Sharma (Editor), Evapotranspiration from plant communities. Elsevier, Amsterdam.

Sui, H., Zeng, D. and Chen, F., 1992. A numerical model for simulating the temperature and moisture regimes of soil under various mulches. Agric. For. Meteorol., 61: 281–299.

Sun, S., 1982. Moisture and heat transport in a soil layer forced by atmospheric conditions. M.Sc. thesis, University of Connecticut, Storrs, CT.

Ten Berge, H.F.M., 1990. Heat and water transfer in bare topsoil and the lower atmosphere. Center for Agricultural Publishing and Documentation (Pudoc), Wageningen.

Van Bavel, C.H.M. and Hillel, D.I., 1976. Calculating potential and actuary evaporation from a bare soil surface by simulation of concurrent flow of water and heat. Agric. Meteorol., 17: 453–476.

Waggoner, P.E., Miller, P.M. and De Roo, H.C., 1960. Plastic Mulching, Bulletin 634. Connecticut Experiment Station, New Haven, CT.

Williams, J.R., Dyke, P.T., Fuchs, W.W., Benson, V.W., Rice, O.W., and Taylor, E.D., 1990. EPIC—Erosion/Productivity Impact Calculator: 2. User Manual. In: A.N. Sharpley and J.R. Williams (Editors), Technical Bulletin No. 1768. US Department of Agriculture, 127 pp.